SRF CAVITY HIGH-GRADIENT STUDY AT 805 MHZ FOR PROTON AND OTHER APPLICATIONS*

T. Tajima#, A. Bhatty, P. Chacon, R. Edwards, G. Eremeev, F. Krawczyk, R. Roybal, J. Sedillo, LANL, Los Alamos, NM 87545, U.S.A.
W. Clemens, P. Kneisel, R. Manus, R. Rimmer, L. Turlington, TJNAF, Newport News, VA 23606, U.S.A.

Abstract

805 MHz elliptical Superconducting RF (SRF) cavities have been used for SNS as the first application for protons. At LANL, R&D started to explore a capability of getting high-gradient cavities (40-50 MV/m) at this frequency for the future applications such as proton and muon based interrogation testing facility added to the LANSCE accelerator and a power upgrade of the LANSCE accelerator for the fission and fusion material test station. Optimized cell designs for "standard", "low-loss" and "re-entrant" shapes as well as the first test result of a "standard" single-cell cavity are presented.

INTRODUCTION

The LANSCE accelerator at LANL produces 800 MeV protons. While presently it consists of normal conducting copper structures, SRF cavities are considered to be added or to replace copper structures for future projects requiring higher-energy/power protons such as active interrogation and fission/fusion material test station. For active interrogation of special nuclear materials, the accelerator needs to be small enough to be deployed in a ship or an aircraft. In order to realize the size reduction with SRF cavities, developing high-gradient cavities is essential. Here, we report our effort to design, fabricate and test 805 MHz SRF cavities to boost the energy of LANSCE accelerator for a land-based demonstration.

CAVITY DESIGN

In order to be able to directly compare with 1.3 GHz high-gradient cavities, we chose β=1. We decided to design 3 shapes, i.e., standard, "low-loss" (LL) and "re-entrant" (RE), following the effort made for the International Linear Collider (ILC) high-gradient alternatives.

Table 1 summarizes the RF parameters after optimization. The primary focus of optimization was to reduce the B_{peak}/E_{acc} as much as possible.

Table 1: A summary of RF design parameters optimized for high gradients. Three shapes, standard (STD), low-loss (LL) and re-entrant (RE) have been designed. The last 3 rows are the ILC cavity design parameters for comparison.

	Frequency	Ep/Ea	Bp/Ea	R/Q	k	G	G*R/Q
	[MHz]		[mT/MV/m]	[Ω]	%	[Ω]	[Ω^2]
Single Cells:							
STD	805.00	1.82	3.75	129.99	N/A	279	36287.1
LL	804.99	2.27	3.60	135.39	N/A	283	38273.9
RE	805.08	2.17	3.57	136.11	N/A	285	38727.1
Inner Cells:							
STD	805.59	2.11	3.81	126.38	1.51	279	35275.1
LL	805.00	2.50	3.63	132.16	1.57	283	37399.0
RE	805.00	2.39	3.58	132.65	1.78	285	37813.3
ILC STD	1300	1.98	4.15	113.8	1.90	271	30839.8
ILC LL	1300	2.36	3.61	133.7	1.52	284	37970.8
ILC RE	1300	2.21	3.76	126.8	1.80	277	35123.6

CAVITY FABRICATION

Due to a budget constraint, we decided to fabricate two standard-shape single-cell cavities in collaboration with Jlab. So far, one cavity has been fabricated from 3.5 mm fine-grain RRR 250 niobium sheets. LANL fabricated most of the forming dies and machining fixtures and JLab formed and electron-beam welded the cavity.

SURFACE TREATMENT

The cavity was immersed in a typical BCP solution, i.e., a mixture of $HF:HNO_3:H_3PO_4$ (1:1:2 volume) solution at <15 °C to remove ~150 μm on the inside and outside surfaces.

Unfortunately, the surfaces facing downward got rough with a number of small ditches probably caused by the hydrogen bubbles moving upward on the surface. Figures 1 and 2 show such surfaces.

*Work supported by DTRA
#tajima@lanl.gov

Figure 1: Outside surface after BCP of 150 μm. This side was facing downward when BCP was done. Traces of bubbles are clearly seen. The surface facing upward was smooth.

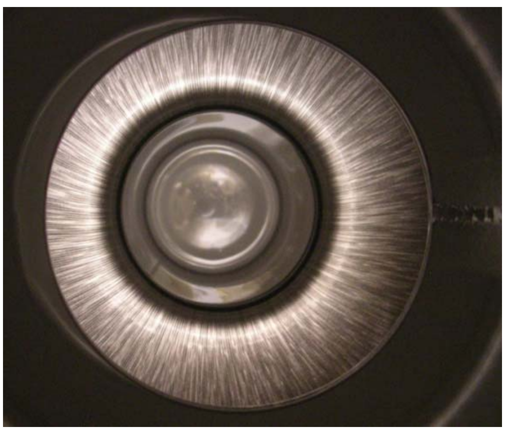

Figure 2: The cavity inside surface after BCP. This side was facing downward during BCP. The surface looked similar to Figure 1.

Figure 3 shows the inside surface that was facing upward. This surface looked like a typical BCPed surface.

Figure 3: The cavity inside surface after BCP. This side was facing upward during BCP.

After BCP, the cavity was high-pressure rinsed with ultra-pure water at 1000 psi for 2 hours in a class 100 clean room and dried with the ports left open overnight. The cavity was then dressed with stainless steel flanges with couplers and a valve. After the procedure in the clean room, the cavity was moved outside and set onto the cryostat insert. The cavity was then connected to the vacuum line and pumped down with a 30 L/s ion pump. Before cooling down, the cavity was baked at 120 ˚C for 41 hours. The cavity vacuum before cooling down was ~1.5E-8 Torr.

TEST PREPARATION

A vacuum port and a remotely-controlled movable coupler were attached to the cavity from the bottom. Figure 4 shows the cavity before being moved to a 38-inch diameter, 10-foot deep vertical cryostat. In order to detect cavity heating, fixed-type temperature mapping boards at every 10 degrees with 37 sensors per board were prepared. We used a diode 1N4148 as a temperature sensor with a custom-made holder similar to the one fabricated for Allen-Bradley resistors used for 1.3 GHz 9-cell cavities [1].

After being moved into the cryostat, the cavity was pre-cooled overnight by filling the liquid nitrogen layer of the cryostat.

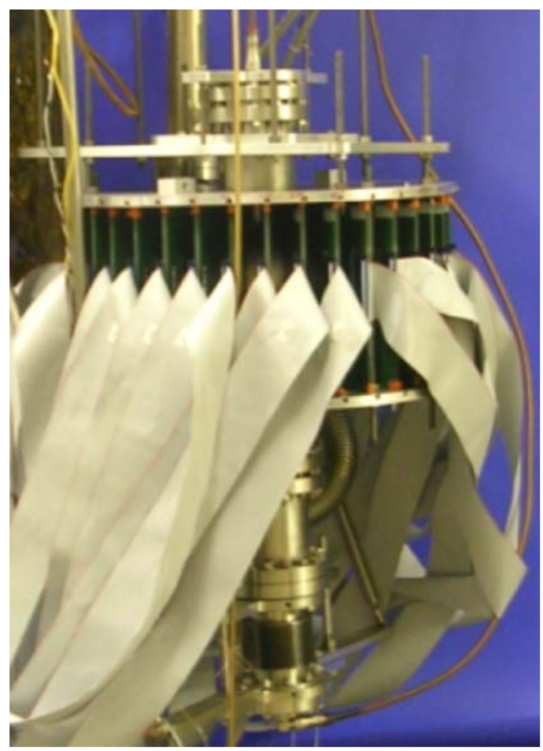

Figure 4: The 805 MHz single-cell cavity surrounded by temperature mapping boards.

TEST RESULTS

The cavity was tested at 4 K (atmospheric pressure at Los Alamos) and 1.5 K (the lowest temperature reached after ~3 hours of pumping). The resonant frequencies at room temperature, 3.97 K and 1.76 K were 805.6058 MHz

[2], 806.2396 MHz and 806.3905 MHz, respectively.

Figure 5 shows the Q_0-E_{acc} curves at 4 K and 1.5 K. The cavity suffered from field emission as we expected from the rough surface, although it did not quench up to 20-25 MV/m, indicating that direct heating with defects are absent up to this level.

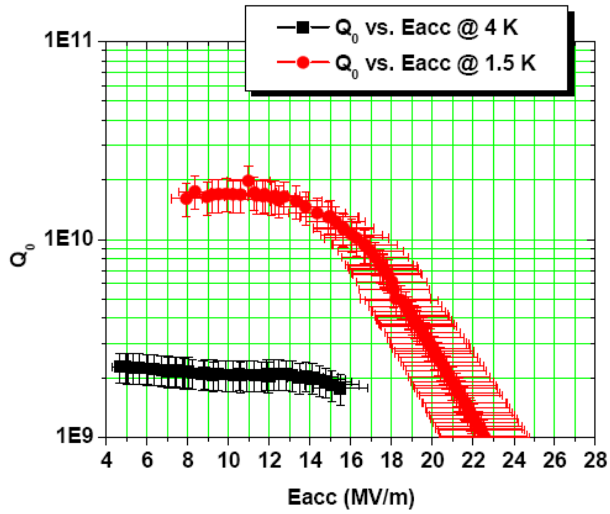

Figure 5: Q_0-E_{acc} curve of the 805 MHz single cell cavity.

TEMPERATURE MAPPING

Prior Diode Tests

The phenomenon that the forward current that a diode allows to flow is dependent on the temperature was used to detect the temperature change. Figure 6 shows the circuit used for the testing.

To select a diode that has an appropriate sensitivity at the temperatures of interest (<10K), four diodes 1N4148, 1N3731, 1N3070 and 1N454 were tested and 1N4148 was selected. Figure 7 shows the temperature dependence of the voltage drop across the diodes when a forward voltage 5 V was applied. As one can see, the diode 1N4148 showed a linear dependence with dV/dT = -0.75 V/K.

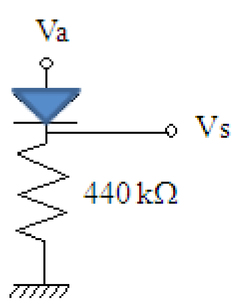

Figure 6: Diode test circuit.

Cavity Test

Thirty-six printed circuit boards (PCBs) with 37 sensors each were attached to cover every 10 degrees in azimuthal direction. For 2D T-mapping, the data taking system developed for a 1.3 GHz 9-cell cavity was modified and the data were divided into 3 sectors, i.e., every 120˚.

Unfortunately, however, since the noise level was higher than the signal level, we were unable to properly detect the temperature rise associated with the field emission.

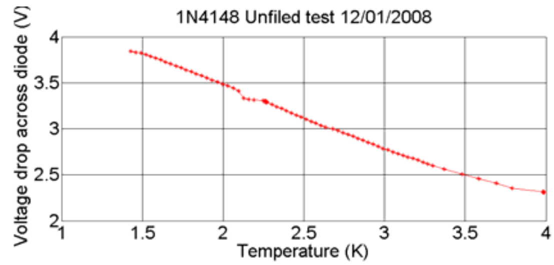

Figure 7: Temperature dependence of the voltage drop across diode 1N4148 when 5 V was applied at V_a in Fig. 6.

A noise level of 0.2-0.25 V has been measured as shown in Fig. 8. This corresponds to a temperature rise of ~0.3 K.

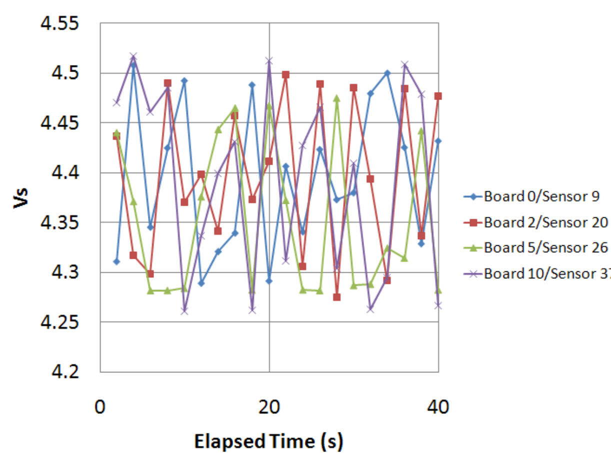

Figure 8: T-map noise level of 4 sensors measured at 4 K. The horizontal axis corresponds to the data number. The data taking time per sector is 2 s.

FUTURE PLAN

The following are the items planned.

- Solve the T-mapping noise problem
- Improve the BCP system
- Try electro-polish the cavity and compare the results (if funding gets available)

REFERENCES

[1] A. Canabal et al., "Full Real-Time Temperature Mapping System for 1.3 GHz 9-cell Cavities," EPAC'08, Genoa, June 2008, p. 841 (2008); http://www.JACoW.org.

[2] P. Kneisel, measured at JLab.